Geotech. Eng., Christchurch, New Zealand.
Kaklamanos, J., and Bradley, B. A. (2016). "Improving our understanding of 1D site response model behavior: physical insights for statistical deviations from 114 KiK-net sites." *2016 Annual Meeting of the Seismological Society of America (SSA)*, Reno, NV (abstract printed in *Seismol. Res. Lett.*, 87, 494).
Kaklamanos, J., Bradley, B. A., Thompson, E. M., and Baise, L. G. (2013). "Critical parameters affecting bias and variability in site response analyses using KiK-net downhole array data." *Bull. Seism. Soc. Am.*, 103, 1733–1749.
Kaklamanos, J., Baise, L. G., Thompson, E. M., and Dorfmann, L. (2015). "Comparison of 1D linear, equivalent-linear, and nonlinear site response models at six KiK-net validation sites." *Soil Dynam. Earthq. Eng.*, 69, 207–219.
Kaklamanos, J., Bradley, B. A., Moolacattu, A. N., and Picard, B. M. (2017). "Adjustments to small-strain damping and soil profile assumptions to improve site response predictions." *2017 SSA Annual Meeting*, Denver, CO (abstract printed in *Seismol. Res. Lett.*, 88, 537).
Kim, B., and Hashash, Y. M. A. (2013). "Site response analysis using downhole array recordings during the March 2011 Tohoku-Oki earthquake and the effect of long-duration ground motions." *Earthq. Spectra*, 29, S37–S54.
Kramer, S. L. (1996). *Geotechnical Earthquake Engineering*. Prentice Hall, Upper Saddle River, NJ.
Li, G., Motamed, R., and Dickenson, S. (2018). "Evaluation of one-dimensional multi-directional site response analyses using geotechnical downhole array data in California and Japan." *Earthq. Spectra*, in press.
Lin, Y.-C., Joh, S.-H., and Stokoe, K. H. (2014). "Interpretation of in-situ tests – some insights." *Geo-Congress 2014 Technical Papers: Geo-Characterization and Modeling for Sustainability*, Atlanta, Georgia, ASCE Geotechnical Special Publication No. 234, M. Abu-Farsakh, X. Yu, and L. R. Hoyos (eds.), 830–839.
Matasović, N., and Vucetic, M. (1993). "Cyclic characterization of liquefiable sands." *J. Geotech. Eng.*, 119, 1805–1822.
Okada, Y., Kasahara, K., Hori, S., Obara, K., Sekiguchi, S., Fujiwara, H., and Yamamoto, A. (2004). "Recent progress of seismic observations networks in Japan – Hi-net, F-net, K-net and KiK-net." *Earth Planets Space*, 56, xv-xxviii.
Ordóñez, G. A. (2017). "SHAKE2000: A computer program for the 1-D analysis of geotechnical earthquake engineering problems." *User's Manual*, GeoMotions, LLC, Lacey, WA.
Phillips, C., and Hashash, Y. M. A. (2009). "Damping formulation for nonlinear 1D site response analyses." *Soil Dynam. Earthq. Eng.*, 29, 1143–1158.
Teague, D. P., and Cox, B. R. (2016). "Site response implications associated with using non-unique Vs profiles from surface wave inversion in comparison with other commonly used methods of accounting for Vs uncertainty." *Soil. Dynam. Earthq. Eng.*, 91, 87–103.
Thompson, E. M., Baise, L. G., Tanaka, Y., and Kayen, R. E. (2012). "A taxonomy of site response complexity." *Soil Dynam. Earthq. Eng.*, 41, 32–43.
Toro, G. R. (1995). "Probabilistic models of site velocity profiles for generic and site-specific ground-motion amplification studies." *Technical Report No. 779574*, Brookhaven National Laboratory, Upton, NY.
Zalachoris, G., and Rathje, E. M. (2015). "Evaluation of one-dimensional site response techniques using borehole arrays." *J. Geotech. Geoenviron. Eng.*, 10.1061/(ASCE)GT.1943-5606.0001366, 04015053.

Zhang, J., Andrus, R. D., and Juang, C. H. (2005). "Normalized shear modulus and material damping ratio relationships." *J. Geotech. Geoenv. Eng.*, 131, 453–464.

Insights into Large-Strain Site Response from Downhole Array Data

Boqin Xu[1] and Ellen Rathje[2]

[1]Dept. of Civil, Architectural, and Environmental Engineering, Univ. of Texas at Austin, TX 78712. E-mail: boqinxu@utexas.edu
[2]Warren S. Bellows Professor, Dept. of Civil, Architectural, and Environmental Engineering, Univ. of Texas at Austin, TX 78712. E-mail: e.rathje@mail.utexas.edu

ABSTRACT

Equivalent linear (EQL) site response analysis commonly overdamps the ground response when the induced shear strains are large. The goal of this paper is to study the methods that can improve the performance of EQL site response predictions for large-intensity motions. The methods include modification of the modulus reduction curve to be consistent with an appropriate shear strength and scaling of the high frequency components of motion to be consistent with an appropriate spectral decay parameter (κ_0). Downhole array data from the IBRH11 site within the Kik-Net network in Japan is used in this study. This site is selected because of the availability of large intensity motions at the site and the presence of softer soils within the profile. The strength correction of the modulus reduction curve reduces the induced shear strains and improves the site response prediction at frequencies close to the natural site frequency. Combining the strength correction with a κ_0 correction increases the high-frequency components of motion and improves the site response prediction of PGA and short period spectral accelerations.

INTRODUCTION

Equivalent-linear (EQL) site response analysis is used to model one-dimensional shear wave propagation and simulates the nonlinear soil response by using strain-compatible soil properties in a linear elastic, frequency domain analysis. One major issue with EQL analysis is the overdamping of the site response when the input motion intensity is large and significant shear strains are induced (e.g., Zalachoris and Rathje 2015). One reason for this overdamping is that the shear strength implied by the modulus reduction curve may be unrealistically small, which leads to excessively large strains being induced. This problem is caused by the fact that modulus reduction curves commonly are derived from laboratory tests with maximum shear strains of about 0.1–0.3%, and the extrapolation of these curves to larger strains using a hyperbolic model does not consider the implied shear strength (Hashash et al. 2010).

EQL analysis can provide better estimates of site response if the modulus reduction curves are corrected to model an appropriate shear strength. Additionally, the spectral decay parameter (κ_0) can be used to constrain the high frequency components of motion to further improve the EQL site response prediction. This paper uses data from the IBRH11 downhole array from the Kiban Kyoshin (Kik-net) network in Japan to investigate how these different modifications to EQL analysis improve site response predictions.

MODIFICATIONS TO EQUIVALALENT LINEAR SITE RESPONSE ANALYSIS FOR LARGE STRAINS

Strength Correction

A modulus reduction curve can be modified at larger strains to be consistent with a target shear strength, as discussed by Hashash et al. (2010). The shear stress-shear strain relationship of a given soil layer can be related to its density, shear wave velocity, and the modulus reduction curve using:

$$\tau = \rho \cdot V_s^2 \cdot \left(\frac{G}{G_{max}}\right)_\gamma \cdot \gamma \quad (1)$$

where τ is the shear stress, ρ is the mass density, V_s is the shear wave velocity, $\left(\frac{G}{G_{max}}\right)_\gamma$ is the $\frac{G}{G_{max}}$ value at shear strain level γ, and γ is the shear strain.

Using the initial modulus reduction curve and shear wave velocity specified for a layer, equation (1) is used to develop an implied shear stress-shear strain curve for the soil. The maximum shear stress in the curve (i.e., strength) is compared with a target shear strength for the soil. For granular materials the target shear strength is defined through a friction angle and vertical effective stress, and for fine-grained materials the target shear strength is defined through an undrained shear strength. If the shear strength obtained from equation (1) is different than the target shear strength, the modulus reduction curve at shear strains larger than 0.1% is adjusted to match the target shear strength. For EQL analysis, the new modulus reduction curve is used directly in the analysis.

κ_0 Correction

Anderson and Hough (1984) introduced κ_0 as a spectral decay factor to model the exponential decay of the Fourier Acceleration Spectrum (FAS) of acceleration at high frequencies:

$$A(f) = A_0 * e^{-\pi \kappa_0 f} \quad (2)$$

where A indicates the Fourier amplitude and f is frequency. For this model, the decay of the FAS is linear in log A versus f space with a slope of $-\pi\kappa_0$. Thus, κ_0 can be used to constrain the high frequency components of motion and their decay with frequency.

Most research related to κ_0 has focused on its relationship to V_{s30} as derived from low intensity motions (e.g., Chandler et al. 2006, Edwards et al. 2011, Van Houtte et al. 2011). Target values of small-strain κ_0 have been used to constrain the small strain damping profiles for use in site response analyses. Durward et al. (1996) investigated κ_0 of low and moderate intensity recorded motions and found that it increases somewhat with increasing peak ground velocity (PGV). This increase in κ_0 is consistent with nonlinear soil response, where large strains will induce more damping that will reduce the high-frequency components of motion.

The parameter κ_0 can be used in EQL site response analysis to modify the overdamped high frequency components of motion when large strains are induced. Given the κ difference ($\Delta\kappa$),

defined as the difference between target κ_0 and the κ_0 of the predicted surface motion from EQL analysis, the surface FAS from EQL is modified by a frequency-dependent scale factor equal to $\exp(-\pi \cdot \Delta\kappa \cdot f)$. The modified FAS is then used to compute the surface ground motion.

UNCORRECTED SITE RESPONSE PREDICTIONS

The downhole array site IBRH11 from the Kik-net strong-motion network in Japan is analyzed to study the empirical site response at small and large strains. IBRH11 has a sensor at the surface and at a depth of 103 m, and the velocity profile at the site is shown in Figure 1. The V_{s30} of the site is 242 m/s. The site response model uses the shear wave velocity profile from Figure 1 and modulus reduction and damping curves from Darendeli (2001). Separate curves were assigned to each velocity layer in Figure 1 using the associated confining pressure at that depth and an assumed plasticity index of 10 and OCR of 1.

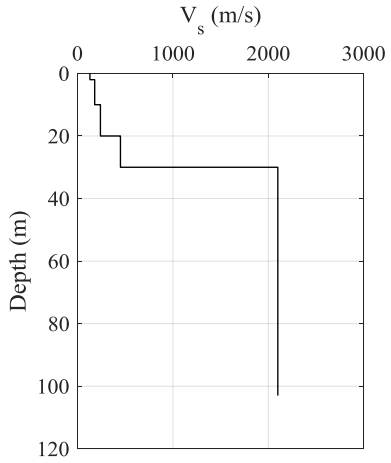

Figure 1. Shear wave velocity profile for IBRH11.

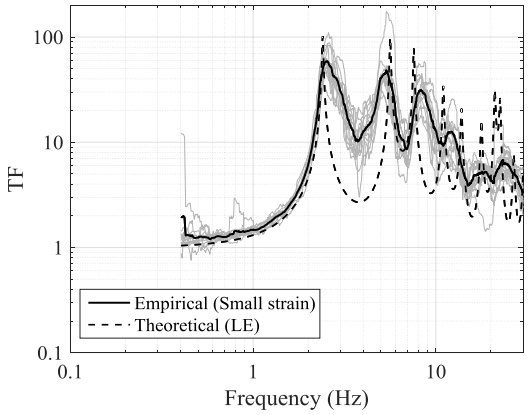

Figure 2. Empirical and theoretical TF for small strain recordings.

To ensure that the response of the IBRH11 site is captured well by 1D analysis, analyses are first performed for low intensity motions where the response will be linear elastic. The strain index ($\gamma_{ind} = PGV_{surf} / V_{s30}$) can provide an apriori estimate of the induced strain, and motions were selected with $\gamma_{ind} < 0.01\%$ to ensure that nonlinear effects were minimized. Additionally,

motions were selected with rupture distances less than 150 km and for $M_w > 3.5$ to ensure robust estimates of κ_0 (Ktenidou et al. 2013). Finally, to ensure signal-to-noise ratios (SNR) larger than about 4, motions were selected that had surface PGA larger than 0.01 g.

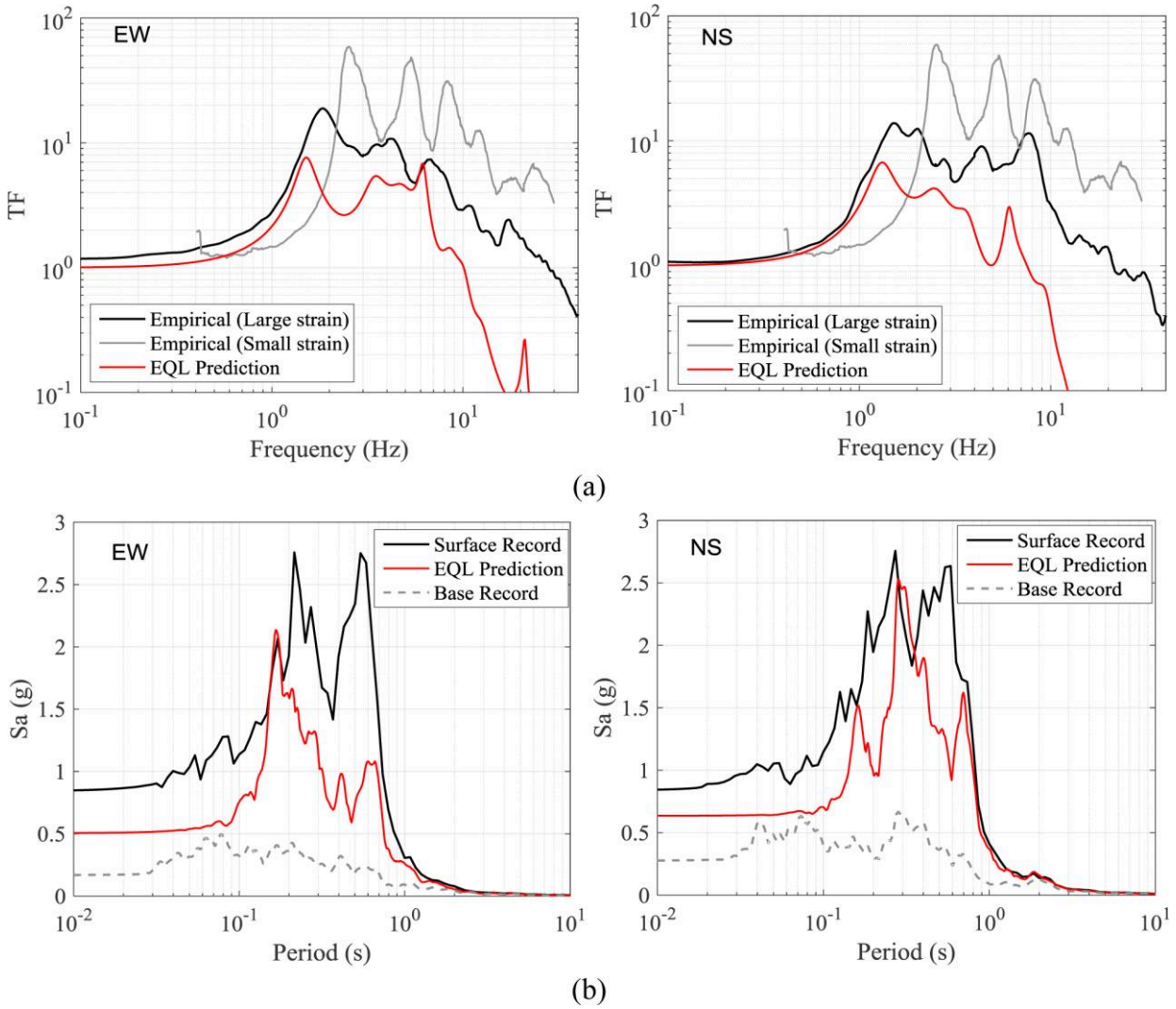

Figure 3. (a) Empirical TF and EQL TF for large strain input motions, (b) predicted and recorded surface response spectra for large strain input motions

The large strain motions used in this analysis represent the two orthogonal components recorded at the site during the Tohoku earthquake (M_w = 8.7). Although the distance to the rupture (R_{rup}) was relatively large at 73 km, the intensity of shaking was significant. The base PGA are 0.17 g (EW) and 0.27 g (NS), and the surface PGA are 0.84 g (EW) and 0.83 g (NS). The strain index is above 0.4% for both components of motion.

The empirical transfer functions (TF) from the small-strain motions are shown in Figure 2. These empirical TF are computed as the ratio of the smoothed FAS from the surface and base sensors. There is a clear first mode peak in the empirical TF at about 2.5 Hz and strong resonances at 5.5 Hz and 8.5 Hz. The theoretical, linear elastic TF computed from a Matlab code verified with Strata (Kottke and Rathje 2008) also shown in Figure 2. The locations of the first

three peaks in the theoretical TF agree well with the empirical TF, although the theoretical amplitudes are larger and the shapes of the peaks are different. Despite these differences, the empirical and theoretical TF in Figure 2 are considered similar based on current criteria (e.g., Thompson et al. 2012).

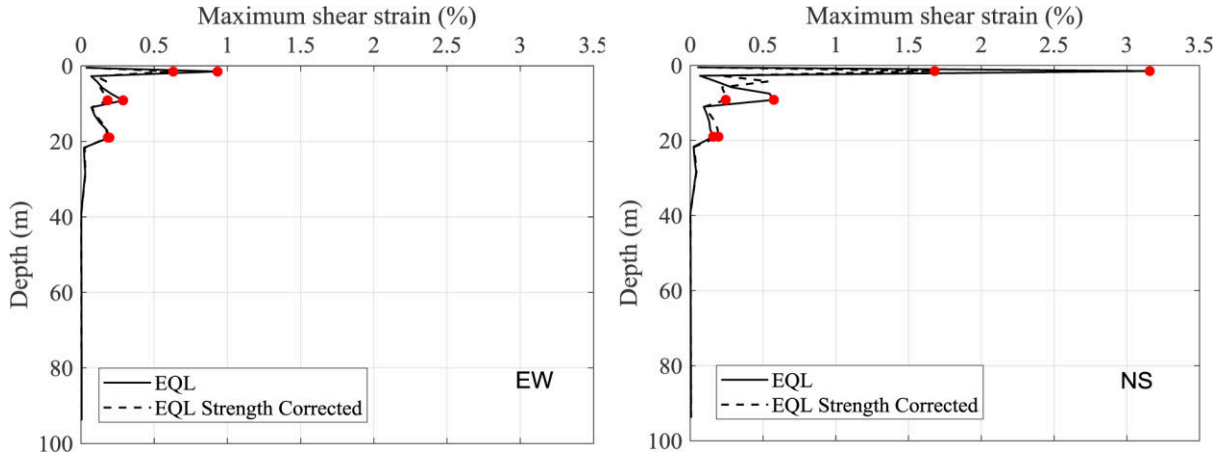

Figure 4. Shear strains induced from original EQL analysis and EQL analysis with the strength corrected modulus reduction curve. Red dots represent peak values.

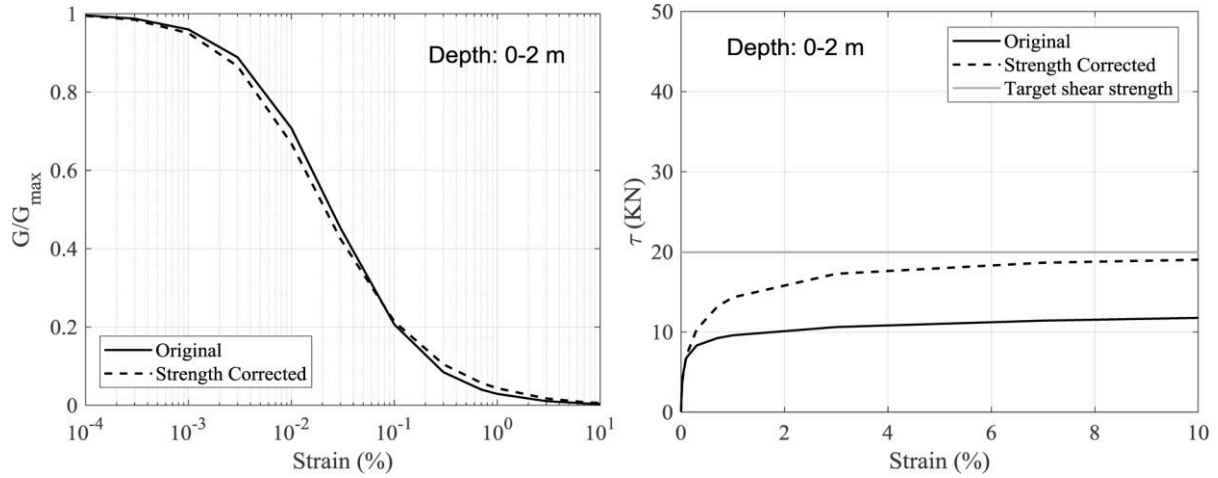

Figure 5. Original and strength corrected modulus reduction curve and stress-strain curve for top layer (0–2 m).

The two horizontal components (EW, NS) of the large strain motions were used as input into separate EQL site response analyses. Figure 3a compares the empirical TF from the large strain recordings with the predicted TF from EQL analysis. The small-strain empirical TF is also shown for reference. The large-strain empirical TF shows that the first mode peak has shifted to about 1.8 Hz from its small-strain value of 2.5 Hz, and the higher frequency peaks have also shifted to smaller values. Additionally, the amplitudes of all three peaks are smaller for the large-strain empirical TF. These changes in TF shape are directly related to the nonlinear response of the soil, which decreases the shear stiffness and associated modal site frequencies and also increases the material damping. The predicted TF from the EQL analysis show similar characteristics as the empirical TF, but the frequencies are shifted more and the amplitudes are smaller. Additionally, at high frequencies the EQL transfer function is smaller than the empirical

TF by factors of 5 to 10. The recorded and predicted surface response spectra are shown in Figure 3b. The predicted motions from EQL analysis are much smaller than recorded, due to the differences in the TF. The predicted PGA are 25% to 40% smaller, and most of the rest of the spectra fall well below the recordings. The shear strains induced in the profile from these two motions are above 0.1% in the top 20 m, with maximum values of about 0.9% for the EW motion and 3.1% for the NS motion.

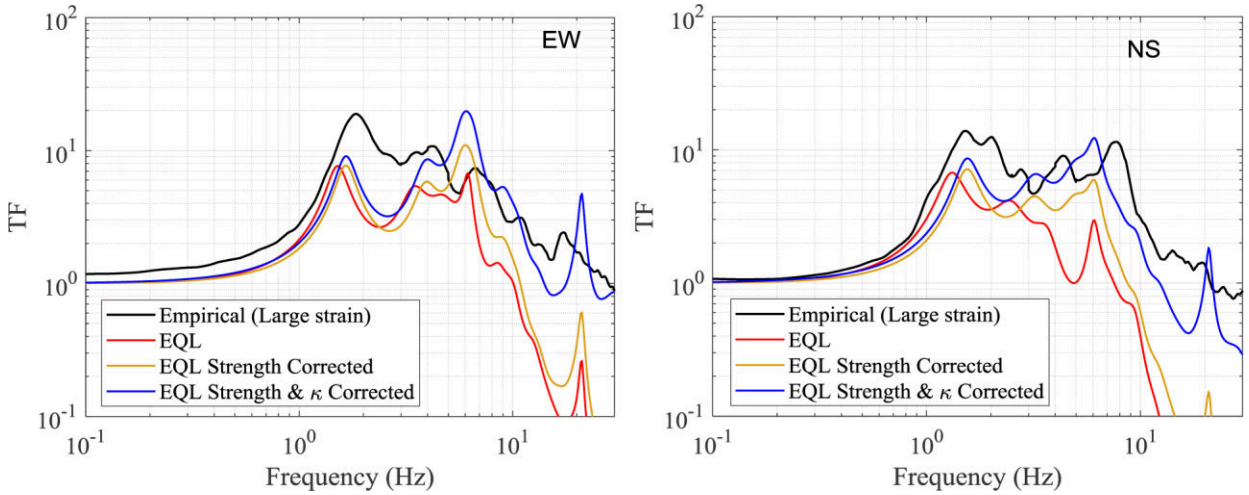

Figure 6. Influence of strength and κ_0 corrections on transfer function from EQL analysis.

INFLUENCE OF STRENGTH AND κ_0 CORRECTION ON SITE RESPONSE PREDICTIONS

The results above show that for large intensity motions, EQL analysis predicts a transfer function with site modal frequencies and amplitudes that are smaller than observed in the empirical TF, which results in an underestimation of the surface acceleration response spectra. The strength correction and κ_0 correction are applied to the EQL analysis of the large strain motions at IBRH11 in an attempt to improve the site response predictions.

The strength correction is applied to the layers that have induced shear strains greater than 0.1%. Figure 4 shows the maximum shear strain profiles from the baseline EQL analysis for the EW and NS motions. The layers with the largest induced shear strains are found in the top 20 m and the strength correction is applied to these four layers (0[0-9]-[0-9]2 m, 2[0-9]-[0-9]5 m, 5[0-9]-[0-9]10 m, and 10[0-9]-[0-9]20 m). Using the shear wave velocity and initial modulus reduction curve of each layer, the implied strength of each layer was estimated. Across these top four layers the implied friction angles are between 14 and 24°, which are significantly smaller than one would expect for the granular soils at the site. For each of these layers, the modulus reduction curves were modified to achieve a target friction angle of 35°. No change was made to the damping curves. The use of the modified modulus reduction curves changed the induced shear strain profile significantly in the top 10 m (Figure 4). The maximum shear strains, which occur close to the ground surface, are reduced to about 0.6% for the EW motion and 1.6% for the NS motion.

Figure 6 shows the TF predicted by EQL analysis for the EW and NS motions using the strength corrected modulus reduction curves. Compared with the original EQL analysis, the first mode peaks are shifted to higher frequencies (~ 2 Hz) due to the smaller strains induced (Figure

4), which results in less softening of the soil stiffness. The locations of the first mode peaks now agree more favorably with the locations of the peaks in the empirical TF. In addition to the shift in modal frequencies, the amplitudes of the TF between 1 and 10 Hz are increased due to the less damping associated with the smaller induced strains. However, the TF are still below the empirical TF for each component of motions, most substantially at high frequencies.

Figure 7 plots the resulting surface response spectra (Sa) and response spectral amplification factors (AF) from the EQL analysis with the strength corrected modulus reduction curves. Compared with the original EQL results the strength corrected responses are larger at all periods less than about 0.6 s, a period range that corresponds with frequencies at or larger than the first mode natural frequency during the shaking. Compared with the empirical (recorded) motions, the strength corrected response in the EW direction still under predicts the Sa and AF around the first mode period of 0.5 s and at periods less than 0.1s, but it over predicts the response at around 0.15 s. This larger response at 0.15 s is due to the larger peak in the EQL strength corrected transfer function for the EW motion at about 6 Hz (Figure 6). This large peak in the EW transfer function may be due to the strain contrast at the top of the profile (Figure 4), where the top layer experiences a maximum strain of about 0.6% and the layer below experiences a strain of about 0.1%. This strain contrast will result in a large velocity contrast that can enhance resonances at the higher modes. For the NS direction, the strength corrected response is more similar to the recording. The Sa and AF agree well between periods of 0.3 and 0.7 s, but the EQL strength corrected prediction is still smaller than the recording at periods less than about 0.3 s. The large response at 0.15 s is not observed in the NS direction because the strain contrast is not as large for this motion (Figure 4).

To better capture the high frequency components of motion, including PGA, a κ_0 correction is applied. As noted previously, κ_0 is related to the slope of the acceleration FAS in log-linear space. The surface FAS from the original EQL analysis displayed κ_0 between 0.09 and 0.1 s for the two components of motion, while the surface recordings displayed κ_0 between 0.05 and 0.06 s. The κ_0 of the surface FAS from the strength corrected EQL analysis are between 0.07 and 0.08 s. These values are smaller than from the original EQL analyses because less damping is induced by the smaller strains, but they are still larger than those from the surface recordings. Thus, a κ_0 correction is applied to the FAS from the strength corrected EQL analysis to adjust the κ_0 to be consistent with a target κ_0 defined from the surface recordings. This correction involves frequency dependent scale factors for the FAS computed as $\exp(-\pi \cdot \Delta\kappa \cdot f)$ where $\Delta\kappa = \kappa_{0,\text{surface recording}} - \kappa_{0,\text{surface EQL}}$.

Figure 6 shows the effect of the κ_0 correction on the transfer functions for the site. The reduction in κ_0 introduced by the κ_0 correction increases the TF amplitudes at frequencies greater than about 2 Hz with the increase largest at the highest frequencies. The strength and κ_0 corrected TF are still generally below the empirical TF, but the differences are reduced. The resulting change in Sa and AF are shown in Figure 7. The κ_0 correction only affects the shorter periods because κ_0 controls high frequency motion. For both the EW and NS components of motion, the strength and κ_0 corrected response improves the agreement with the recordings for PGA and Sa at periods less than 0.1 s. For the EW component, the κ_0 correction results in a further over estimation of the response at around 0.15 s and no real improvement at the site

period of about 0.5 s. For the NS component of motions, the κ_0 correction generates a response very similar to the surface recording across all frequencies.

An interesting observation from Figure 7 is the significantly different AF at IBRH11 for the recordings in the two orthogonal directions. Both components of motion indicate a first mode period of about 0.5 s, but the AF at this period is 12 in the EW direction while it is about 9 in the NS direction. This difference may indicate that a factor other than one-dimensional site response is influencing the motions, such as three-dimensional velocity variations. Of course, the two orthogonal components of motion do not act independently of one another during earthquake shaking, despite the fact that the EQL analyses presented here assume that they do. Nonetheless, this observation demonstrates that it is difficult to judge a large strain site response prediction from a single component of motion because it may be influenced by other factors not taken into account in the analysis.

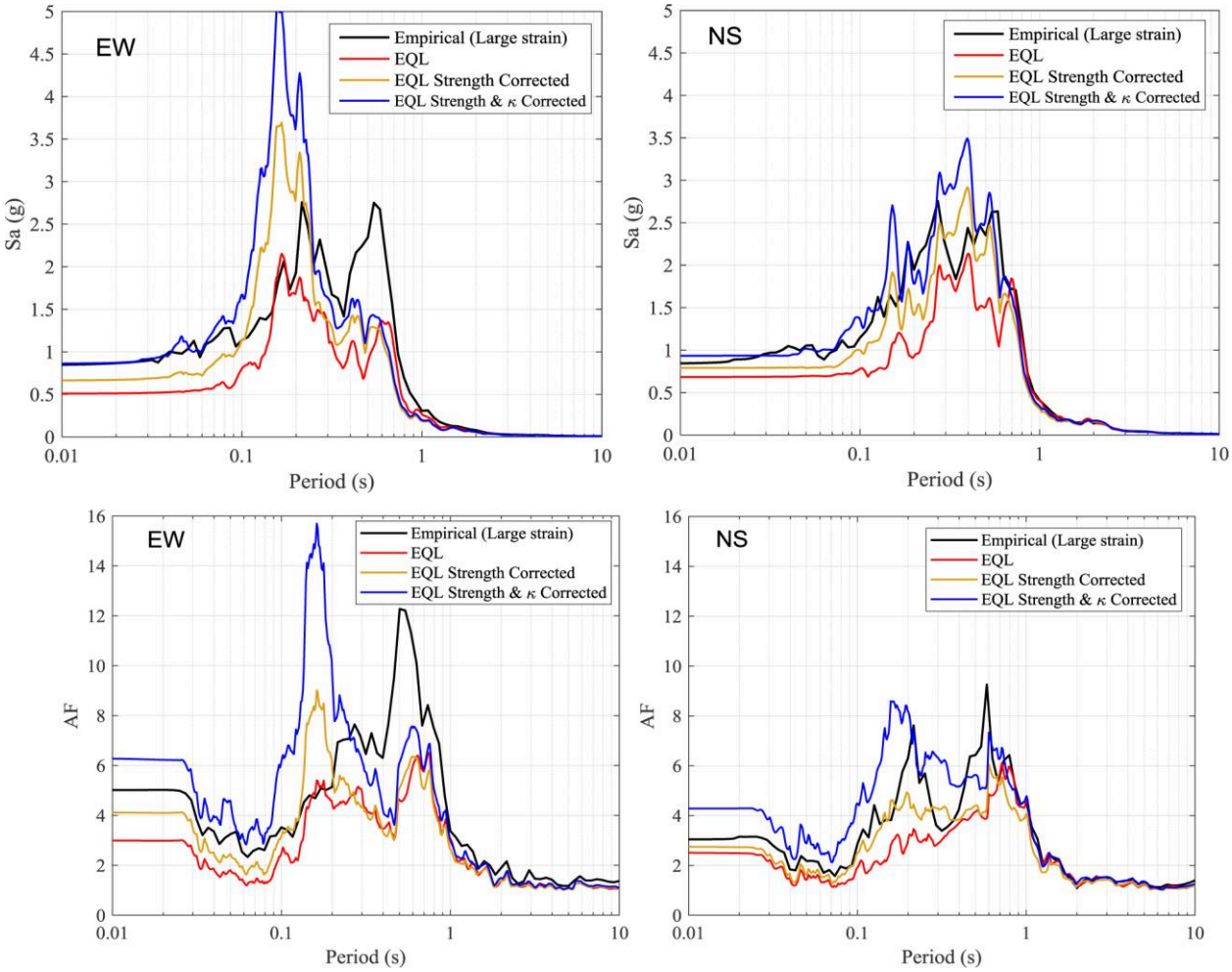

Figure 7. Influence of strength correction and κ_0 correction on surface response spectra spectral amplification factor from EQL analysis.

CONCLUSIONS

Equivalent linear (EQL) analysis commonly overdamps site response when the input motion is intense and the induced shear strains are large. In this study, methods to improve the